


Competition of ANN and RSM techniques in predicting the behavior of the CuO-liquid paraffin

Yacine Khetib^{a,b} , Hala M. Abo-Dief^c, Abdullah K. Alanazi^c, Muhyaddin Rawa^{b,d}, S. Mohammad Sajadi^{e,f}, and Mohsen Sharifpur^{g,h}

^aMechanical Engineering Department, Faculty of Engineering, King Abdulaziz University, Jeddah, Saudi Arabia; ^bCenter Excellence of Renewable Energy and Power, King Abdulaziz University, Jeddah, Saudi Arabia; ^cDepartment of Chemistry, College of Science, Taif University, Taif, Saudi Arabia; ^dDepartment of Electrical and Computer Engineering, Faculty of Engineering, King Abdulaziz University, Jeddah, Saudi Arabia; ^eDepartment of Nutrition, Cihan University-Erbil, Kurdistan Region, Iraq; ^fDepartment of Phytochemistry, SRC, Soran University, KRG, Iraq; ^gDepartment of Mechanical and Aeronautical Engineering, University of Pretoria, Pretoria, South Africa; ^hDepartment of Medical Research, China Medical University Hospital, China Medical University, Taichung, Taiwan

ABSTRACT

In this article, the estimation of CuO-liquid paraffin nanofluid viscosity was assessed using response surface method (RSM) and artificial neural network (ANN) methods. Since CuO-liquid paraffin nanofluid is Newtonian, two parameters of temperature and mass fraction were introduced in ANN and RSM techniques at 25–100 °C, 0.25–6 wt.%. Both methods map the three-dimensional input space to one-dimensional space (viscosity). A response surface cubic model was approved by applying ANOVA and calculations showed an R^2 value of 0.923 and a maximum margin of deviation of 10.482%. Efforts revealed that ANN with five neurons takes precedence over others. The R^2 and maximum deviation margin were 0.994, and 3.266%, respectively. Finally, the comparison of ANN and RSM methods indicated that the ANN method is more accurate than the RSM for conducting the nanofluid viscosity. The accuracy of ANN was such that for 50% of points, MOD was less than 1%. For MOD in the range of 0–2%, 90% of points can be predicted with an error of less than 2%. This figure for RSM was only 37%.

KEYWORDS

Artificial neural network; CuO; nanofluid; paraffin; response surface methodology; viscosity

Introduction

The need for energy in various sectors is a growing trend that brings with it major problems such as air pollution and carbon dioxide emissions (Jahangiri et al. 2016, 2019, 2020; Pahlavan et al. 2018; Mostafaeipour et al. 2020). In addition, the shortage of fossil energy resources must be incorporated. Reducing energy consumption in various sectors, especially in the building and industry sectors should be on the agenda of researchers and in this regard, many studies have been conducted (Jahangir et al. 2018; Mahdavi, Garbadeen, et al. 2019; Mahdavi, Sharifpur, et al. 2019; Menni et al. 2020; Giwa et al. 2020a, 2020b). Applying energy storage technique can lead to energy saving. Phase change materials (PCMs) store a lot of energy when undergoes the phase change process and

consequently can be used as the main candidate in this regard (Bayat, Faridzadeh, and Toghraie 2018; Dardir et al. 2019; Miansari et al. 2020; Ho et al. 2021). These materials have been used in various sectors such as buildings (Nariman, Kalbasi, and Rostami 2021), cooling (Yang et al. 2019; Zhang et al. 2019; Abdollahi and Rahimi 2020; Aqib et al. 2020; Chen et al. 2020), solar collectors (El Khadraoui et al. 2017; Abuşka, Şevik, and Kayapınar 2019; Algarni et al. 2020; Palacio, Rincón, and Carmona 2020), etc. The major challenge in using PCMs is their low thermal conductivity (Rathore and Shukla 2019; Rostami, Afrand, et al. 2020; Yang, Huang, and Zhou 2020), which causes incomplete or long-delayed phase change. Since nanoparticles have increased the thermal conductivity and thermal performance of base fluids, nanofluid seem to perform better alongside

CONTACT Yacine Khetib  ykhetib@yahoo.com  Mechanical Engineering Department, Faculty of Engineering, King Abdulaziz University, Jeddah 80204, Saudi Arabia; Mohsen Sharifpur  mohsen.sharifpur@up.ac.za  Department of Mechanical and Aeronautical Engineering, University of Pretoria, Pretoria 0002, South Africa.

© 2021 Taylor & Francis Group, LLC

nanoparticles (Motamedi, Eskandari, and Yeganeh 2012; Motamedi, Mashhadi, and Rastgoo 2013; Motamedi et al. 2018; Gomari et al. 2019; Abad et al. 2020; Alizadeh, Dorfaki, et al. 2020; Alizadeh, Mohebbi Najm Abad, et al. 2020; Motamedi, Naghdi, and Jalali 2020; Valizadeh Ardalan et al. 2020; Alizadeh, Abad, Ameri, et al. 2021; Alizadeh, Abad, Fattahi, et al. 2021; Alizadeh, Mesgarpour, et al. 2021; Mesgarpour et al. 2021).

In a study conducted by Yan, Kalbasi, Karimipour, et al. (2021) it was found that adding MWCNT boosted $k_{Paraffin}$ up to 40.86%. The study on viscosity of paraffin in the presence of MWCNT was performed by Liu et al. (2020). Although the viscosity behavior of paraffin was Newtonian, MWCNTs nanoparticles, in addition to changing it to non-Newtonian, increased the viscosity by up to 86%. Colla et al. (2017) inserted carbon black as well as Al_2O_3 into paraffin and revealed that $k_{Paraffin}$ intensified up to 25%. They affirmed that Al_2O_3 has less positive effects on $k_{Paraffin}$ than carbon black. Ramakrishnan et al. (2017) added exfoliated graphene nano-platelets to paraffin by 1 vol.% and found that $k_{Paraffin}$ boosted up to 49%. Lin and Al-Kayiem (2016) loaded expanded graphite into Paraffin wax led to amplification in $k_{Paraffin}$ by 14% and 46.3% at 0.5 and 2 wt.%. Hussain et al. (2017) added carbon nano-sheets to composite PCM (combination of oleic and capric acid) and revealed that $k_{composite PCM}$ boosted by 55% at 0.1 wt.%. The use of linear (Milani Shirvan et al. 2016; Hatami and Jing 2017; Kalbasi et al. 2019; Hemmat Esfe and Sadati Tilebon 2020) and nonlinear regression methods (Longo et al. 2012; Toghraie et al. 2019; Nguyen et al. 2020; Sadeghi et al. 2020) has been used by many researchers to determine whether the use of this technique can be advantageous in extracting results without performing further experimentation. Hemmat Esfe, Kiannejad Amiri, and Bahiraei (2019) applied the RSM technique on $k_{SiO_2/water}$ and $\mu_{SiO_2/water}$ to navigate the parameters of $\frac{k_{SiO_2/water}}{k_{water}}$ and $\frac{\mu_{SiO_2/water}}{\mu_{water}}$ at 1–5 vol.%. Based on R^2 , it was found that the R^2 for the former and latter one was 0.9952 and 0.9971, respectively. Iranmanesh et al. (2016) used RSM to navigate $\frac{k_{Gr/water}}{k_{water}}$ and $\frac{\mu_{Gr/water}}{\mu_{water}}$. Introducing of T, VF and nanoparticles specific as

the input parameters, they proved that R^2 for the former and latter one is 0.9925 and 0.9619, respectively. Hemmat Esfe and Motallebi (2019) applied the RSM technique on the measured experimental results for $k_{Al/oil}$ and $\mu_{Al/oil}$, and affirmed these parameters were predictable with an R^2 values of 0.9734 and 0.9914, respectively. In another study, Milani Shirvan et al. (2017) used RSM to derive a mathematical correlation for evaluation of mean Nusselt number and heat exchanger effectiveness. Based on the R^2 criteria, for the former and latter parameters, the R^2 was reported to be 0.9993 and 0.8501, respectively (Table 1).

Experimental data

In this research, the results of the experimental study conducted by Ghasemi and Karimipour (2018) were investigated to examine the usefulness of applying RSM and ANN. The authors produced many nanofluid samples containing CuO and liquid paraffin to study the nanofluid rheological behavior. The authors performed a TEM test for evaluating the CuO molecules structures and after dispersing them into the paraffin, conducted DLS test and affirmed that the nanoparticles diameter was within the 30 to 40 nm which implies that the suspension can be considered as nanofluid. To ensure the stability of CuO/paraffin, zeta potential test was performed and it was found that the critical zeta potential was not within the -30 to 30 mV. They conclude that the prepared samples at 0.25 to 6 wt.% were stable. They measured $\mu_{CuO/paraffin}$ by Brookfield viscometer (DV2T) at $25-100$ °C and $10-160$ $\frac{1}{s}$. They showed that $\mu_{CuO/paraffin}$ did not follow the non-Newtonian behavior, hence temperature and volume fraction are the main input parameters. The experimental measurements were illustrated in Figure 1.

Regression-based methods

Among the various numerical approaches studied by various researchers (Afrand et al. 2015; Karimi and Afrand 2018; Guthrie, Torabi, and Karimi 2019; Hunt et al. 2019; Saeed et al. 2019; Christodoulou et al. 2020; Habib et al. 2020; Kalbasi 2021). Regression is a set of statistical

Table 1. Applications of ANN and RSM in forecasting nanofluid properties.

References	Output parameter	Findings	Technique
Tian, Kalbasi, Qi, et al. (2020)	$\frac{k_{Al_2O_3-MWCNT/10w40}}{k_{10w40}}$	R^2 , MSE and MOD_{max} were 0.9948, 0.0008485 and 0.97%, $R^2 = 0.972$	RSM
Rostami, Kalbasi, Sina, et al. (2021)	$\frac{k_{MWCNT/paraffin}}{k_{paraffin}}$	$R^2 = 0.982$ $MSE = 8.194 \times 10^{-8}$ $MOD = 1.608\%$ $R^2 = 0.9877$ $MSE = 1.122 \times 10^{-5}$ $MOD = 0.7\%$ $R^2 = 0.988$ $RMSE = 2.1613$ $MOD = 7.25\%$	RSM
Tian, Kalbasi, Jahanshahi, et al. (2020)	$\frac{\sigma_{Gr/EG}}{\sigma_{Gr}}$	$R^2 = 0.982$ $MSE = 8.194 \times 10^{-8}$ $MOD = 1.608\%$ $R^2 = 0.9877$ $MSE = 1.122 \times 10^{-5}$ $MOD = 0.7\%$ $R^2 = 0.988$ $RMSE = 2.1613$ $MOD = 7.25\%$	RSM
Alsarraf et al. (2021)	$\frac{\sigma_{ZnO-SiO_2/EG-water}}{\sigma_{EG-water}}$	$R^2 = 0.982$ $MSE = 8.194 \times 10^{-8}$ $MOD = 1.608\%$ $R^2 = 0.9877$ $MSE = 1.122 \times 10^{-5}$ $MOD = 0.7\%$ $R^2 = 0.988$ $RMSE = 2.1613$ $MOD = 7.25\%$	RSM
Rostami, kalbasi, Jahanshahi, et al. (2020)	Consistency index for evaluating $\mu_{SiO_2/EG}$	$R^2 = 0.982$ $MSE = 8.194 \times 10^{-8}$ $MOD = 1.608\%$ $R^2 = 0.9877$ $MSE = 1.122 \times 10^{-5}$ $MOD = 0.7\%$ $R^2 = 0.988$ $RMSE = 2.1613$ $MOD = 7.25\%$	RSM
Rostami, kalbasi, Jahanshahi, et al. (2020)	Power law index for evaluating $\mu_{SiO_2/EG}$	$R^2 = 0.982$ $MSE = 8.194 \times 10^{-8}$ $MOD = 1.608\%$ $R^2 = 0.9877$ $MSE = 1.122 \times 10^{-5}$ $MOD = 0.7\%$ $R^2 = 0.988$ $RMSE = 2.1613$ $MOD = 7.25\%$	RSM
Rostami, Kalbasi, Talebkeikhah, et al. (2021)	$\frac{k_{MWCNT-TiO_2/EG}}{k_{EG}}$	$R^2 = 0.982$ $MSE = 8.194 \times 10^{-8}$ $MOD = 1.608\%$ $R^2 = 0.9877$ $MSE = 1.122 \times 10^{-5}$ $MOD = 0.7\%$ $R^2 = 0.988$ $RMSE = 2.1613$ $MOD = 7.25\%$	RSM
Yan, Kalbasi, et al. (2021a)	$\mu_{MWCNTs-TiO_2/EG}$	ANFIS method was slightly better than the SVM one. $R^2 = 0.993$	ANN
Rostami, Kalbasi, Sina, et al. (2021)	$\frac{k_{MWCNT/paraffin}}{k_{paraffin}}$	$R^2 = 0.997$ $MSE = 5.568 \times 10^{-6}$ $MOD < 1\%$ $R^2 = 0.986$ $MSE = 5.068 \times 10^{-8}$ $MOD = 1.427\%$ $R^2 = 0.9992$ $RMSE = 0.0015$ $MOD = 0.785\%$ $R^2 = 0.999$	ANN
Yan, Kalbasi, et al. (2021b)	$\frac{\sigma_{MWCNT/paraffin}}{\sigma_{paraffin}}$	$R^2 = 0.997$ $MSE = 5.568 \times 10^{-6}$ $MOD < 1\%$ $R^2 = 0.986$ $MSE = 5.068 \times 10^{-8}$ $MOD = 1.427\%$ $R^2 = 0.9992$ $RMSE = 0.0015$ $MOD = 0.785\%$ $R^2 = 0.999$	ANN
Tian, Kalbasi, Jahanshahi, et al. (2020)	$\frac{\sigma_{Gr/EG}}{\sigma_{Gr}}$	$R^2 = 0.997$ $MSE = 5.568 \times 10^{-6}$ $MOD < 1\%$ $R^2 = 0.986$ $MSE = 5.068 \times 10^{-8}$ $MOD = 1.427\%$ $R^2 = 0.9992$ $RMSE = 0.0015$ $MOD = 0.785\%$ $R^2 = 0.999$	ANN
Rostami, Kalbasi, Talebkeikhah, et al. (2021)	$\frac{k_{MWCNT-TiO_2/EG}}{k_{EG}}$	$R^2 = 0.997$ $MSE = 5.568 \times 10^{-6}$ $MOD < 1\%$ $R^2 = 0.986$ $MSE = 5.068 \times 10^{-8}$ $MOD = 1.427\%$ $R^2 = 0.9992$ $RMSE = 0.0015$ $MOD = 0.785\%$ $R^2 = 0.999$	ANN
Li et al. (2020)	$\frac{\mu_{MgO-water}}{\mu_{water}}$	$R^2 = 0.997$ $MSE = 5.568 \times 10^{-6}$ $MOD < 1\%$ $R^2 = 0.986$ $MSE = 5.068 \times 10^{-8}$ $MOD = 1.427\%$ $R^2 = 0.9992$ $RMSE = 0.0015$ $MOD = 0.785\%$ $R^2 = 0.999$	ANN

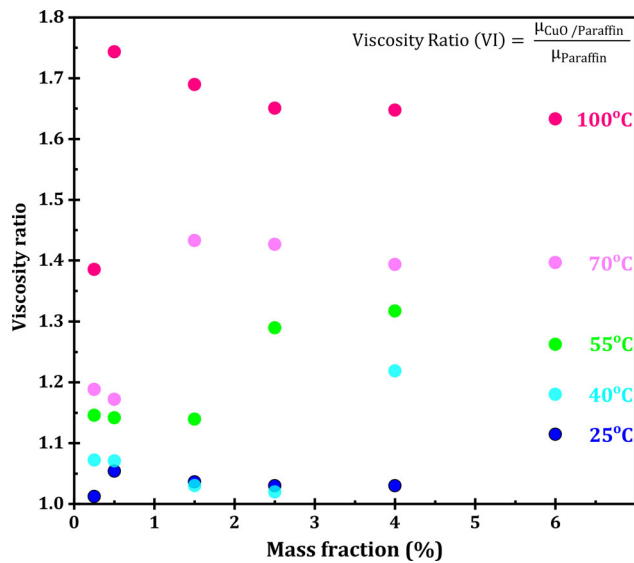


Figure 1. Viscosity ratio variation for nanofluid (Ghasemi and Karimpour 2018).

computations that try to establish a correlation between input and output parameters. In the simplest case, the correlation is linear and with increasing complexity, second-order, third-order

regression as the linear combination can be used. In nonlinear regression, correlations are more complex. One of the most complex correlations between input and output variables is created by an artificial neural network. An artificial neural network (ANN) is a computing machine based on animal brains (Esfé et al. 2018; Hemmat Esfe et al. 2018). ANN consists of several computational units called neurons in which neurons together form an interconnected network. The connection of neurons in the living organism's neural network is based on synapses, while in the artificial neural network it is based on the signal. Each neuron receives a signal (or real number) and performs calculations on it using mathematical functions. In other words, neurons receive input signals from previous neurons and convert them into a new signal for subsequent neurons. Neural networks consist of three layers called input, hidden and output. The first layer consists of several neurons (exactly equal to the number of independent input parameters) in which each

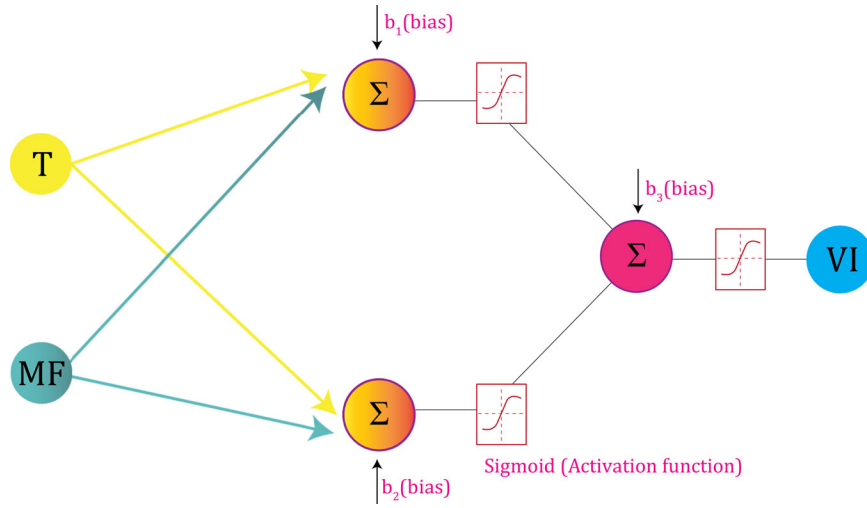


Figure 2. ANN structure ($VI = \frac{\mu_{CuO/Paraffin}}{\mu_{Paraffin}}$).

Table 2. Linear, quadratic and cubic polynomial coefficients.

Linear	Quadratic	Cubic
a_0 0.94735	b_0 0.94910	c_0 1.0175
a_1 0.59272	b_1 0.32839	c_1 -0.14683
a_2 2.2756	b_2 6.4576	c_2 2.4423
	b_3 -0.032810	c_3 21.744
	b_4 0.26091	c_4 0.93635
	b_5 -68.377	c_5 -100.84
		c_6 -8.3632
		c_7 -217.86
		c_8 -0.31782
		c_9 1387.3

neuron receives its independent parameter data. The neurons in the first layer do not alter the input information, in other words, they receive input data and then transmit it to the second layer (hidden layer). In this study, viscosity is dependent on temperature (T) and nanoparticles mass fraction (MF), hence they are considered as the independent parameters. Temperature data is received by a neuron and the other neuron store the mf data. Temperature and volume fraction data (as shown in Figure 1) transmit to each neuron in the middle layer. These neurons process information and produce a signal (real number). The number of neurons in this layer is not known and the user must determine it by trial and error. In this study, the output parameter refers to the viscosity ratio ($\frac{\mu_{CuO/Paraffin}}{\mu_{Paraffin}}$), and since the number of neurons in the last layer is equal to the output parameters number, a neuron is assigned to ($\frac{\mu_{CuO/Paraffin}}{\mu_{Paraffin}}$). Now the output parameter is compared with the exact value (experimental) to examine the accuracy neural network

accuracy. By changing the number of neurons and the type of mathematical function in the hidden layer, the user can greatly improve the accuracy (Figure 2).

Response surface methodology (RSM) is a set of statistical computations in which it is tried to establish a linear combination between the input parameters and output. For ANN, although the output can be more than one variable, but for RSM method, a unique correlation is established for each output. In other words, two output variables cannot be estimated by providing a unique correlation. Considering the input parameters of T and MF and output ($\frac{\mu_{CuO/Paraffin}}{\mu_{Paraffin}}$), several polynomial functions containing a linear combination of T and MF were proposed. Using mathematical criteria, the polynomial with most closely fits the data, will be chosen by the user.

$$\mu_{nf} = a_0 + a_1T + a_2(MF) \quad (1)$$

$$\mu_{nf} = b_0 + b_1T + b_2(MF) + b_3T(MF) + b_4T^2 + b_5(MF)^2 \quad (2)$$

$$\mu_{nf} = c_0 + c_1T + c_2(MF) + c_3T(MF) + c_4T^2 + c_5(MF)^2 + c_6T^2(MF) + c_7T(MF)^2 + c_8T^3 + c_9(MF)^3 \quad (3)$$

In this study, through calculating of R^2 , the margin of deviation (MOD) and mean square error (MSE), the accuracy of regression-based methods were evaluated (Rostami, Kalbasi, Jahanshahi, et al. 2020; Tian, Kalbasi, Jahanshahi,

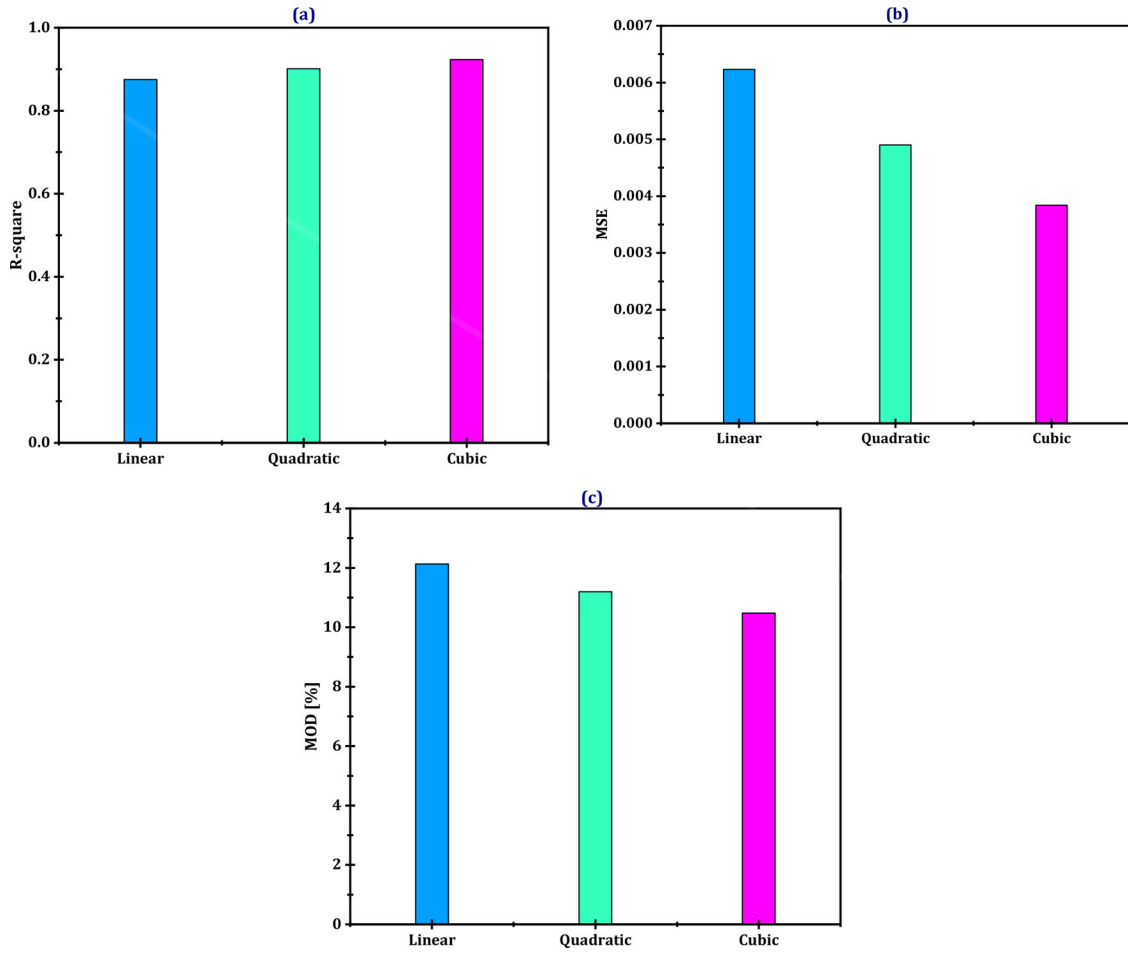


Figure 3. Statistical parameters for linear, quadratic and cubic and their comparison.

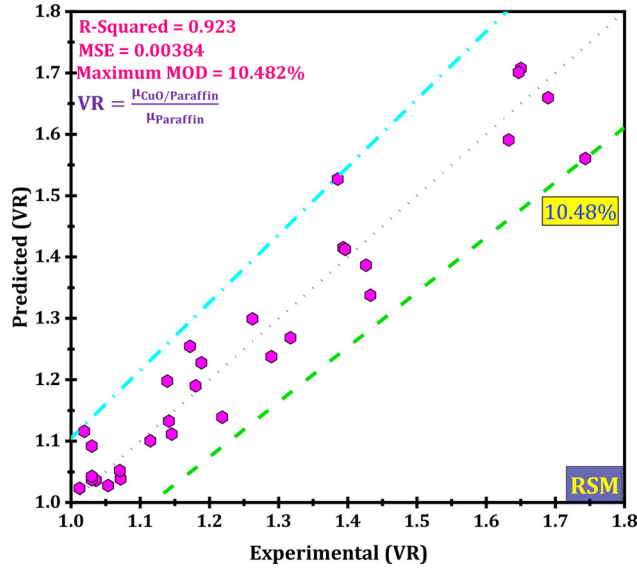


Figure 4. Viscosity ratio for RSM and comparison with experimental data.

et al. 2020; Rostami, Kalbasi, Talebkeikhah, et al. 2021; Yan, Kalbasi, et al. 2021b).

$$MSE = \frac{1}{24} \sum_{i=1}^{24} \left(\left[\frac{\mu_{CuO/Paraffin}}{\mu_{Paraffin}} \right]_{Pred} - \left[\frac{\mu_{CuO/Paraffin}}{\mu_{Paraffin}} \right]_{Exp} \right)^2 \quad (4)$$

$$R^2 = \left(\frac{\sum_{i=1}^{24} \left(\left[\frac{\mu_{nf}}{\mu_{bf}} \right]_{Exp} - \left[\frac{\mu_{nf}}{\mu_{bf}} \right]_{Exp} \right) \left(\left[\frac{\mu_{nf}}{\mu_{bf}} \right]_{Pred} - \left[\frac{\mu_{nf}}{\mu_{bf}} \right]_{Pred} \right)}{\sqrt{\sum_{i=1}^{24} \left(\left[\frac{\mu_{nf}}{\mu_{bf}} \right]_{Exp} - \left[\frac{\mu_{nf}}{\mu_{bf}} \right]_{Exp} \right)^2} \sqrt{\sum_{i=1}^N \left(\left[\frac{\mu_{nf}}{\mu_{bf}} \right]_{Pred} - \left[\frac{\mu_{nf}}{\mu_{bf}} \right]_{Pred} \right)^2}} \right)^2$$

$$\frac{\mu_{CuO/Paraffin}}{\mu_{Paraffin}} = \frac{\mu_{nf}}{\mu_{bf}} \quad (5)$$

$$MOD = \frac{\left[\frac{\mu_{CuO/Paraffin}}{\mu_{Paraffin}} \right]_{Exp} - \left[\frac{\mu_{CuO/Paraffin}}{\mu_{Paraffin}} \right]_{Pred}}{\left[\frac{\mu_{CuO/Paraffin}}{\mu_{Paraffin}} \right]_{Exp}} \times 100 \quad (6)$$

Results

As mentioned in the previous section, regression-based techniques can be used to establish the correlation between T and MF as independent input parameters and $\frac{\mu_{CuO/Paraffin}}{\mu_{Paraffin}}$ as an output parameter.

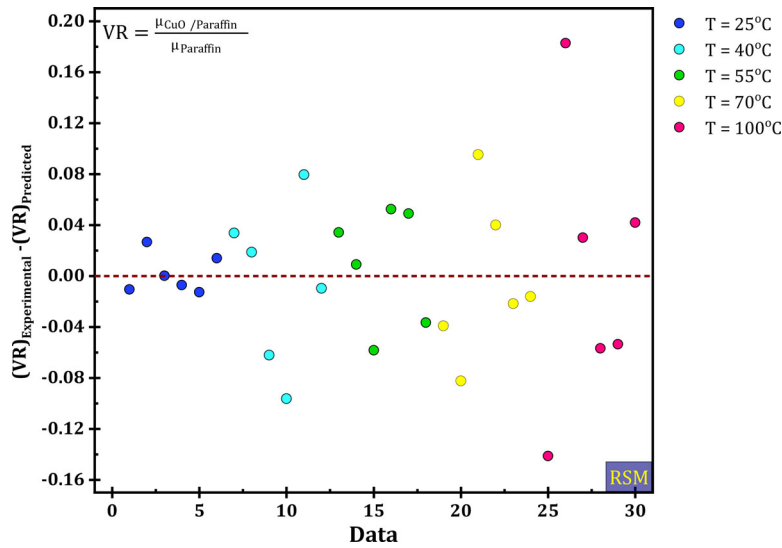


Figure 5. Residual values for RSM technique.

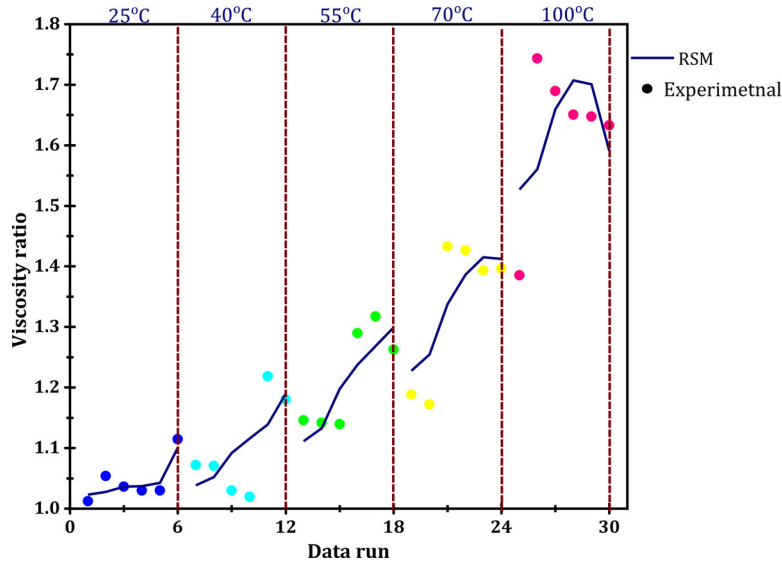


Figure 6. Laboratory and numerical values of viscosity ratio $\frac{\mu_{CuO/Paraffin}}{\mu_{Paraffin}}$ for RSM technique.

Applying statistical calculations, the linear (Equation (1)), quadratic (Equation (2)) and cubic (Equation (3)) polynomial coefficients were determined and recorded in Table 2.

The R^2 criteria can be used to select the most appropriate polynomial. It shows the correlation between T , MF and $\frac{\mu_{CuO/Paraffin}}{\mu_{Paraffin}}$ and the closer it is to one, the more desirable it is. To calculate R^2 , we can refer to Equation (5). At best, if $\left[\frac{\mu_{CuO/Paraffin}}{\mu_{Paraffin}}\right]_{Exp}$ and $\left[\frac{\mu_{CuO/Paraffin}}{\mu_{Paraffin}}\right]_{Num}$ are the same for all points, the R^2 value is equal to one, in which case there is no error. Therefore, MSE and MOD parameters will not have values greater than zero.

However, the statistical indicators for linear, quadratic and cubic polynomials are illustrated in Figure 3. Focusing on Figure 3 reveals that the cubic polynomial has the most appropriate R^2 , while MSE and MOD parameters for it are much closer to the ideal conditions (zero value), indicating the superiority of cubic polynomial over linear as well as quadratic ones.

If R-square is equal to unity, it means that $\left[\frac{\mu_{CuO/Paraffin}}{\mu_{Paraffin}}\right]_{Exp}$ and $\left[\frac{\mu_{CuO/Paraffin}}{\mu_{Paraffin}}\right]_{Num}$ are the same, and so if they are plotted on a graph, they form a bisector line (Figure 4). Figure 3 affirmed that although the cubic case was the most appropriate

polynomial correlation, the accuracy of the cubic polynomial is not high. In particular, Figure 3(c) illustrated that the maximum MOD for cubic one is 10.48%, which is far from the desired value.

One of the best methods to evaluate the accuracy of regression-based methods is to analyze the residual value. The residual value (i.e., $\left[\frac{\mu_{\text{CuO/Paraffin}}}{\mu_{\text{Paraffin}}} \right]_{\text{Exp}} - \left[\frac{\mu_{\text{CuO/Paraffin}}}{\mu_{\text{Paraffin}}} \right]_{\text{Num}}$) for the RSM method is illustrated in Figure 5, and as can be seen, there is a large scatter relative to the ideal line (zero line) which indicates that cubic polynomial (RSM) cannot be used to predict $\frac{\mu_{\text{CuO/Paraffin}}}{\mu_{\text{Paraffin}}}$.

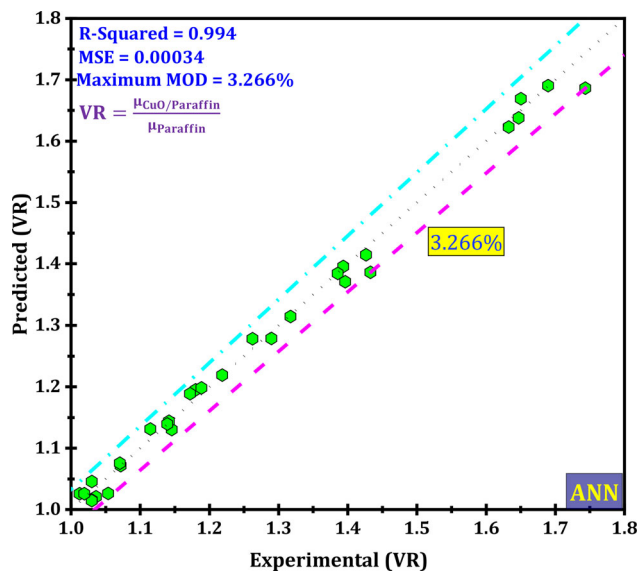


Figure 7. Viscosity ratio for ANN and comparison with experimental data.

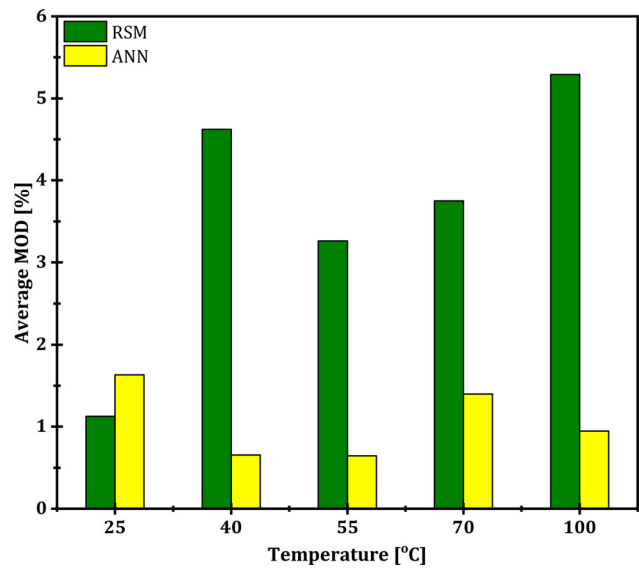


Figure 9. Average MOD for ANN and RSM at each temperature.

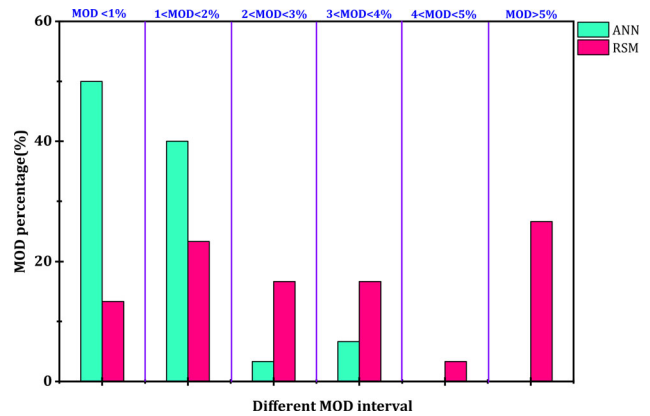


Figure 10. MOD distribution at the various intervals for ANN and RSM.

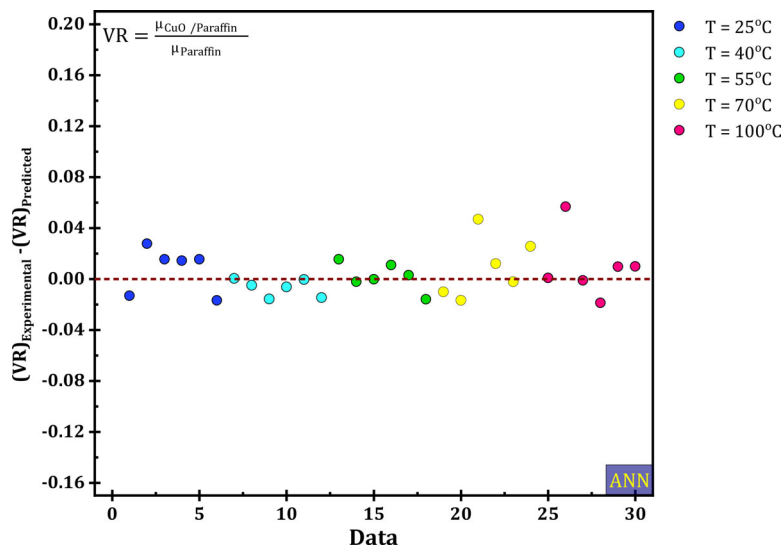


Figure 8. Residual values for ANN technique.

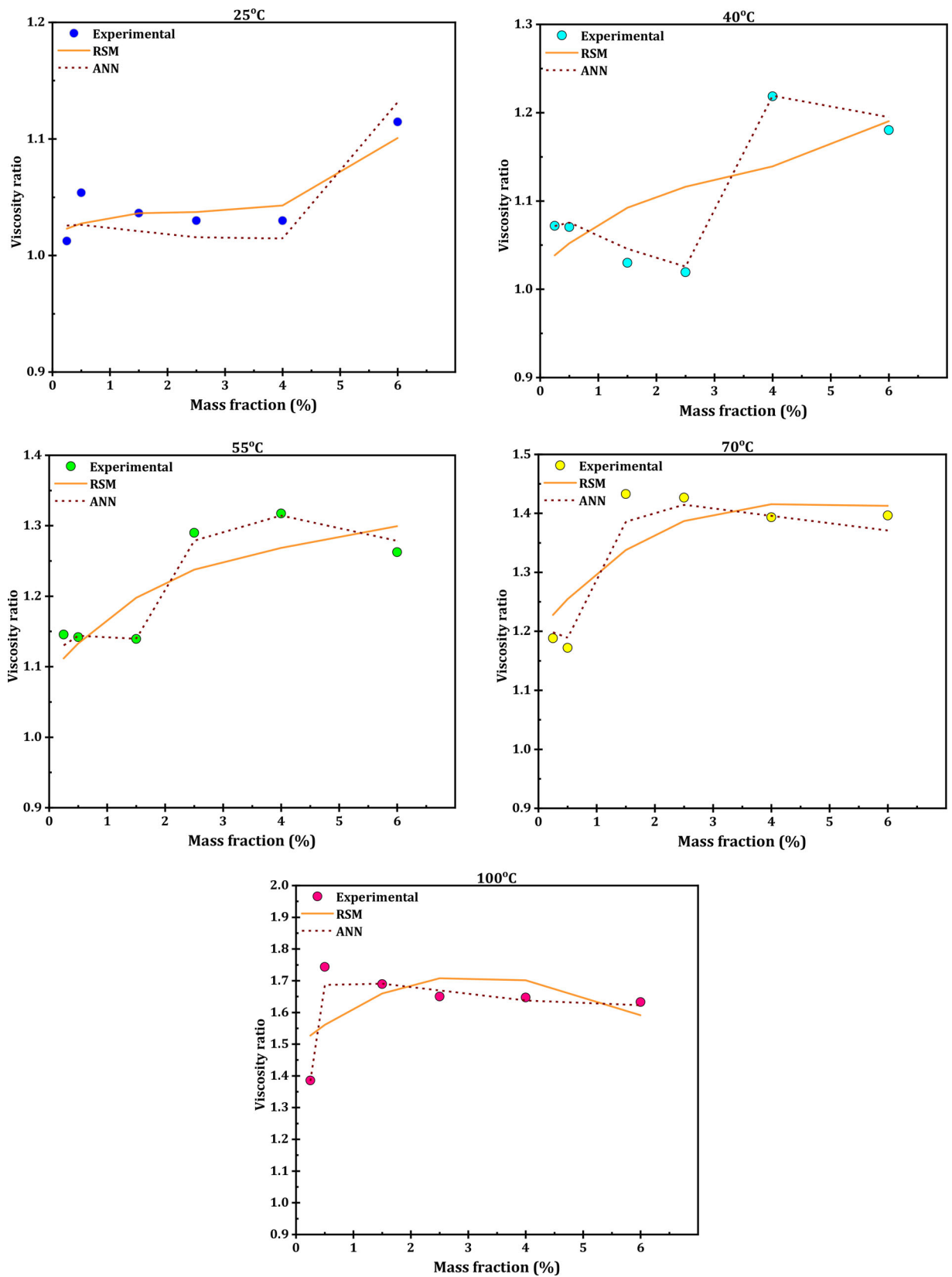


Figure 11. The superiority of the ANN approach over RSM one in estimating the trend of changes in viscosity ratio $\left(\frac{\mu_{CuO/Paraffin}}{\mu_{Paraffin}}\right)$.

with confidence. The next question that needs to be answered is the ability of RSM technique to

predict the chart trend. Hence, Figure 6 is drawn to measure the ability of RSM approach. At

25 °C, this method could predict the trend of $\frac{\mu_{\text{CuO/Paraffin}}}{\mu_{\text{Paraffin}}}$ with insignificant accuracy, while at other temperatures, it could not forecast the trend, so the use of RSM to predict $\frac{\mu_{\text{CuO/Paraffin}}}{\mu_{\text{Paraffin}}}$ is not recommended.

In the following, the ANN technique is evaluated. It has already been mentioned that the usefulness of this method can be improved by trial and error. Therefore, trial and error was performed and it was observed that the neural network based on five neurons in the middle layer is the best case from the perspective of R-square. Note that out of a total of 30 input data points, 22, 4 and 4 points were assigned for train, validation and test. Similar to the RSM method, the deviation of $\left[\frac{\mu_{\text{CuO/Paraffin}}}{\mu_{\text{Paraffin}}}\right]_{\text{Num}}$ from the $\left[\frac{\mu_{\text{CuO/Paraffin}}}{\mu_{\text{Paraffin}}}\right]_{\text{Exp}}$ values are illustrated in Figures 7 and 8.

The scales of Figures 5 and 8 are the same so that they can be compared. For ANN method, the scatter of points is much less, which indicates the higher accuracy of this method than the RSM one. On the other hand, a comparison of Figures 4 and 7 reveals that the ANN method can estimate $\frac{\mu_{\text{CuO/Paraffin}}}{\mu_{\text{Paraffin}}}$ much more. Because it has a higher R^2 as well as less MSE and MOD values

The average MOD at each temperature for ANN and RSM approaches is illustrated in Figure 9. First, at any temperature, the RSM approach accuracy is much lower than ANN one. Second, the scatter of points (according to Figures 5 and 8) is such that no particular trend for average MOD relative to temperature can be imagined.

Figures 4 and 7 proved the deviation of numerical results from the laboratory ones, hence MOD is not equal to zero. In RSM and ANN approaches, MOD is equal to 10.48% and 3.26%, respectively. Figures 4 and 7 reported the maximum MOD value, indicating that at other points, MOD is less than 10.48% (for RSM) and 3.26% (for ANN). The MOD distribution is reported in Figure 10 and it can be seen that for the ANN method, 50% of the input data have a MOD value below 1%. In other words, for half the points, $\left[\frac{\mu_{\text{CuO/Paraffin}}}{\mu_{\text{Paraffin}}}\right]_{\text{Num}}$ differs from $\left[\frac{\mu_{\text{CuO/Paraffin}}}{\mu_{\text{Paraffin}}}\right]_{\text{Exp}}$ by less than 1%. This figure was

40% for MOD within 1 to 2%. It is concluded that for 90% of the input points, the value of $\frac{\mu_{\text{CuO/Paraffin}}}{\mu_{\text{Paraffin}}}$ is less than 2% different from the actual value.

If the MOD value is increased to the range of 0–4%, it can be seen that the neural network has been able to successfully predict all points, while for the RSM method, 70% of the data points have a MOD value less than 4%. Finally, the estimation power of ANN and RSM in forecasting the trend of changes in $\frac{\mu_{\text{CuO/Paraffin}}}{\mu_{\text{Paraffin}}}$ are illustrated in Figure 11. It is clear that the ANN approach is very capable in this field so that its use in estimating $\frac{\mu_{\text{CuO/Paraffin}}}{\mu_{\text{Paraffin}}}$ is acceptable.

Conclusion

In this study, the application of regression-based methods on predicting the viscosity of a conventional PCM-based nanofluid was assessed. Since the rheological behavior of paraffin (base fluid), as well as CuO/paraffin (nanofluid), were Newtonian, hence the results were independent of the shear rate and temperature and mass fraction parameters were known as independent parameters. Regression-based methods were evaluated in both linear and nonlinear modes. The main results were:

1. Implementation of the linear regression was performed by RSM technique and it was observed that the accuracy of the cubic polynomial was higher than the quadratic and linear one.
2. Statistical criteria showed that R^2 , MOD and MSE for the apparent method in the best case, take the values of 0.923, 10.482% and 0.00384, respectively.
3. Trial and error revealed that the middle layer with five neurons provided the best estimation power with $R^2 = 0.994$, MOD = 3.266% and MSE = 0.00034.
4. The accuracy of the neural network was such that for half of the points, the MOD was below 1%. For 90% of the points, there is a maximum of 2% difference between the numerical and laboratory results.

5. For the RSM technique, only 13.3% of the points have an error of less than 1%. This figure was 37% for MOD within 0–2%.
6. The approved neural network forecasted nanofluid viscosity with much higher accuracy. Also, it was able to predict the trend of viscosity changes well. The ANN method is not only unacceptably accurate but also inefficient at predicting the viscosity ratio trend.

Funding

This work was supported by the Taif University Researchers Supporting grant number (TURSP-2020/266) of Taif University, Taif, Saudi Arabia.

ORCID

Yacine Khetib  <http://orcid.org/0000-0003-1466-9584>

References

- Abad JMN, Alizadeh R, Fattahi A, Doranehgard MH, Alhajri E, Karimi N. 2020. Analysis of transport processes in a reacting flow of hybrid nanofluid around a bluff-body embedded in porous media using artificial neural network and particle swarm optimization. *J Mol Liq.* 313: 113492. doi:10.1016/j.molliq.2020.113492
- Abdollahi N, Rahimi M. 2020. Potential of water natural circulation coupled with nano-enhanced PCM for PV module cooling. *Renewable Energy* 147:302–309. doi:10.1016/j.renene.2019.09.002
- Abuşka M, Şevik S, Kayapınar A. 2019. Experimental analysis of solar air collector with PCM-honeycomb combination under the natural convection. *Sol Energy Mater Sol Cells* 195:299–308. doi:10.1016/j.solmat.2019.02.040
- Afrand M, Farahat S, Hossein Nezhad A, Sheikhzadeh GA, Sarhaddi F, Wongwises S. 2015. Multi-objective optimization of natural convection in a cylindrical annulus mold under magnetic field using particle swarm algorithm. *Int Commun Heat Mass Transfer.* 60:13–20. doi:10.1016/j.icheatmasstransfer.2014.11.006
- Algarni S, Mellouli S, Alqahtani T, Almutairi K, Khan A, Anqi A. 2020. Experimental investigation of an evacuated tube solar collector incorporating nano-enhanced PCM as a thermal booster. *Appl Therm Eng.* 180:115831. doi:10.1016/j.applthermaleng.2020.115831
- Alizadeh R, Mohebbi Najm Abad J, Ameri A, Mohebbi MR, Mehdizadeh A, Zhao D, Karimi N. 2021. A machine learning approach to the prediction of transport and thermodynamic processes in multiphysics systems - heat transfer in a hybrid nanofluid flow in porous media. *J Taiwan Inst Chem Eng.* 124:290–306. doi:10.1016/j.jtice.2021.03.043
- Alizadeh R, Mohebbi Najm Abad J, Fattahi A, Mohebbi MR, Doranehgard MH, Li LK, Alhajri E, Karimi N. 2021. A machine learning approach to predicting the heat convection and thermodynamics of an external flow of hybrid nanofluid. *J Energy Resour Technol.* 143(7): 070902. doi:10.1115/1.4049454
- Alizadeh R, Dorfaki V, Ameri A, Valizadeh Ardalan M, Sarafan MJ. 2020. Heat transfer and pressure drop in a sinus blowing of copper oxide-water non-Newtonian nanofluid in a sudden expansion process in the presence of variable magnetic field: a numerical solution. *Energy Sources Part A.* 1–24.
- Alizadeh R, Mesgarpour M, Ameri A, Mohebbi Najm Abad J, Wongwises S. 2021. Artificial intelligence prediction of natural convection of heat in an oscillating cavity filled by CuO nanofluid. *J Taiwan Inst Chem Eng.* 124:75–90. doi:10.1016/j.jtice.2021.04.067
- Alizadeh R, Mohebbi Najm Abad J, Fattahi A, Alhajri E, Karimi N. 2020. Application of machine learning to investigation of heat and mass transfer over a cylinder surrounded by porous media—the radial basic function network. *Trans ASME J Energy Resour Technol.* 142.
- Alsarraf J, Al-Rashed AAAA, Alnaqi AA, Shahsavari Goldanlou A. 2021. Dominance of cohesion of EG-water molecules over Van der Waals force between SiO₂-ZnO nanoparticles in the liquid interface. *Powder Technol.* 379:537–546. doi:10.1016/j.powtec.2020.10.079
- Aqib M, Hussain A, Muhammad Ali H, Naseer A, Jamil F. 2020. Experimental case studies of the effect of Al₂O₃ and MWCNTs nanoparticles on heating and cooling of PCM. *Case Stud Therm Eng.* 22:100753. doi:10.1016/j.csite.2020.100753
- Bayat M, Faridzadeh MR, Toghraie D. 2018. Investigation of finned heat sink performance with nano enhanced phase change material (NePCM). *Thermal Sci Eng Progress* 5:50–59. doi:10.1016/j.tsep.2017.10.021
- Chen F, Huang R, Wang C, Yu X, Liu H, Wu Q, Qian K, Bhagat R. 2020. Air and PCM cooling for battery thermal management considering battery cycle life. *Appl Therm Eng.* 173:115154. doi:10.1016/j.applthermaleng.2020.115154
- Christodoulou L, Karimi N, Cammarano A, Paul M, Navarro-Martinez S. 2020. State prediction of an entropy wave advecting through a turbulent channel flow. *J Fluid Mech.* 882.
- Colla L, Fedele L, Mancin S, Danza L, Manca O. 2017. Nano-PCMs for enhanced energy storage and passive cooling applications. *Appl Therm Eng.* 110:584–589. doi:10.1016/j.applthermaleng.2016.03.161
- Dardir M, Panchabikesan K, Haghghat F, El Mankibi M, Yuan Y. 2019. Opportunities and challenges of PCM-to-air heat exchangers (PAHXs) for building free cooling applications—A comprehensive review. *J Storage Mater.* 22:157–175. doi:10.1016/j.est.2019.02.011
- El Khadraoui A, Bouadila S, Kooli S, Farhat A, Guizani A. 2017. Thermal behavior of indirect solar dryer: Nocturnal usage of solar air collector with PCM. *J Cleaner Prod.* 148:37–48. doi:10.1016/j.jclepro.2017.01.149

- Esfé MH, Esfandeh S, Afrand M, Rejvani M, Rostamian SH. 2018. Experimental evaluation, new correlation proposing and ANN modeling of thermal properties of EG based hybrid nanofluid containing ZnO-DWCNT nanoparticles for internal combustion engines applications. *Appl Therm Eng.* 133:452–463. doi:10.1016/j.applthermaleng.2017.11.131
- Ghasemi S, Karimipour A. 2018. Experimental investigation of the effects of temperature and mass fraction on the dynamic viscosity of CuO-paraffin nanofluid. *Appl Therm Eng.* 128:189–197. doi:10.1016/j.applthermaleng.2017.09.021
- Giwa SO, Sharifpur M, Ahmadi MH, Meyer JP. 2020a. A review of magnetic field influence on natural convection heat transfer performance of nanofluids in square cavities. *J Therm Anal Calorim.* 145(5):2581–2623. doi:10.1007/s10973-020-09832-3
- Giwa SO, Sharifpur M, Ahmadi MH, Meyer JP. 2020b. Magnetohydrodynamic convection behaviours of nanofluids in non-square enclosures: A comprehensive review. *Math Methods Appl Sci.* doi:10.1002/mma.6424
- Gomari SR, Alizadeh R, Alizadeh A, Karimi N. 2019. Generation of entropy during forced convection of heat in nanofluid stagnation-point flows over a cylinder embedded in porous media. *Numerical Heat Transfer Part A: Appl.* 75(10):647–673. doi:10.1080/10407782.2019.1608774
- Guthrie DG, Torabi M, Karimi N. 2019. Energetic and entropic analyses of double-diffusive, forced convection heat and mass transfer in microreactors assisted with nanofluid. *J Therm Anal Calorim.* 137(2):637–658. doi:10.1007/s10973-018-7959-3
- Habib R, Karimi N, Yadollahi B, Doranehgard MH, Li LK. 2020. A pore-scale assessment of the dynamic response of forced convection in porous media to inlet flow modulations. *Int J Heat Mass Transfer* 153:119657. doi:10.1016/j.ijheatmasstransfer.2020.119657
- Hatami M, Jing D. 2017. Optimization of wavy direct absorber solar collector (WDASC) using Al₂O₃-water nanofluid and RSM analysis. *Appl Therm Eng.* 121: 1040–1050. doi:10.1016/j.applthermaleng.2017.04.137
- Hemmat Esfe M, Amiri MK, Bahiraei M. 2019. Optimizing thermophysical properties of nanofluids using response surface methodology and particle swarm optimization in a non-dominated sorting genetic algorithm. *J Taiwan Inst Chem Eng.* 103:7–19. doi:10.1016/j.jtice.2019.07.009
- Hemmat Esfe M, Motallebi SM. 2019. Four objective optimization of aluminum nanoparticles/oil, focusing on thermo-physical properties optimization. *Powder Technol.* 356:832–846. doi:10.1016/j.powtec.2019.08.041
- Hemmat Esfe M, Rostamian H, Esfandeh S, Afrand M. 2018. Modeling and prediction of rheological behavior of Al₂O₃-MWCNT/5W50 hybrid nano-lubricant by artificial neural network using experimental data. *Phys. A* 510: 625–634. doi:10.1016/j.physa.2018.06.041
- Hemmat Esfe M, 2020. and SM. Sadati Tilebon Statistical and artificial based optimization on thermo-physical properties of an oil based hybrid nanofluid using NSGA-II and RSM. *Phys. A* 537: 122126.
- Ho CJ, Lin K-H, Rashidi S, Toghraie D, Yan W-M. 2021. Experimental study on thermophysical properties of water-based nanoemulsion of n-icosane PCM. *J Mol Liq.* 321:114760. doi:10.1016/j.molliq.2020.114760
- Hunt G, Karimi N, Yadollahi B, Torabi M. 2019. The effects of exothermic catalytic reactions upon combined transport of heat and mass in porous microreactors. *Int J Heat Mass Transfer* 134:1227–1249. doi:10.1016/j.ijheatmasstransfer.2019.02.015
- Hussain SI, Dinesh R, Roseline AA, Dhivya S, Kalaiselvam S. 2017. Enhanced thermal performance and study the influence of sub cooling on activated carbon dispersed eutectic PCM for cold storage applications. *Energy Build.* 143:17–24. doi:10.1016/j.enbuild.2017.03.011
- Iranmanesh S, Mehrali M, Sadeghinezhad E, Ang BC, Ong HC, Esmaeilzadeh A. 2016. Evaluation of viscosity and thermal conductivity of graphene nanoplatelets nanofluids through a combined experimental–statistical approach using respond surface methodology method. *Int Commun Heat Mass Transfer* 79:74–80. doi:10.1016/j.icheatmasstransfer.2016.10.004
- Jahangir MH, Ghazvini M, Pourfayaz F, Ahmadi MH, Sharifpur M, Meyer JP. 2018. Numerical investigation into mutual effects of soil thermal and isothermal properties on heat and moisture transfer in unsaturated soil applied as thermal storage system. *Numerical Heat Transfer Part A: Appl.* 73(7):466–481. doi:10.1080/10407782.2018.1449518
- Jahangiri M, Ghaderi R, Haghani A, Nematollahi O. 2016. Finding the best locations for establishment of solar-wind power stations in Middle-East using GIS: A review. *Renewable Sustainable Energy Rev.* 66:38–52. doi:10.1016/j.rser.2016.07.069
- Jahangiri M, Haghani A, Mostafaeipour A, Khosravi A, Raeisi HA. 2019. Assessment of solar-wind power plants in Afghanistan: A review. *Renewable Sustainable Energy Rev.* 99:169–190. doi:10.1016/j.rser.2018.10.003
- Jahangiri M, Shamsabadi AA, Mostafaeipour A, Rezaei M, Yousefi Y, Pomares LM. 2020. Using fuzzy MCDM technique to find the best location in Qatar for exploiting wind and solar energy to generate hydrogen and electricity. *Int J Hydrogen Energy* 45(27):13862–13875. doi:10.1016/j.ijhydene.2020.03.101
- Kalbasi R. 2021. Introducing a novel heat sink comprising PCM and air - Adapted to electronic device thermal management. *Int J Heat Mass Transfer* 169:120914. doi:10.1016/j.ijheatmasstransfer.2021.120914
- Kalbasi R, Afrand M, Alsarraf J, Tran M-D. 2019. Studies on optimum fins number in PCM-based heat sinks. *Energy* 171:1088–1099. doi:10.1016/j.energy.2019.01.070
- Karimi A, Afrand M. 2018. Numerical study on thermal performance of an air-cooled heat exchanger: Effects of hybrid nanofluid, pipe arrangement and cross section. *Energy Convers Manage.* 164:615–628. doi:10.1016/j.enconman.2018.03.038

- Li Y, Kalbasi R, Karimipour A, Sharifpur M, Meyer J. 2020. Using of artificial neural networks (ANNs) to predict the rheological behavior of magnesium oxide-water nanofluid in a different volume fraction of nanoparticles, temperatures, and shear rates. *Math Methods Appl Sci*. doi:10.1002/mma.6418
- Lin SC, Al-Kayiem HH. 2016. Evaluation of copper nanoparticles-Paraffin wax compositions for solar thermal energy storage. *Sol Energy* 132:267–278. doi:10.1016/j.solener.2016.03.004
- Liu X, Mohammed HI, Zarenezhad Ashkezari A, Shahsavari A, Hussein AK, Rostami S. 2020. An experimental investigation on the rheological behavior of nanofluids made by suspending multi-walled carbon nanotubes in liquid paraffin. *J Mol Liq*. 300:112269. doi:10.1016/j.molliq.2019.112269
- Longo GA, Zilio C, Ceseracciu E, Reggiani M. 2012. Application of artificial neural network (ANN) for the prediction of thermal conductivity of oxide-water nanofluids. *Nano Energy* 1(2):290–296. doi:10.1016/j.nanoen.2011.11.007
- Mahdavi M, Garbadeen I, Sharifpur M, Ahmadi MH, Meyer JP. 2019. Study of particle migration and deposition in mixed convective pipe flow of nanofluids at different inclination angles. *J Therm Anal Calorim*. 135(2):1563–1575. doi:10.1007/s10973-018-7720-y
- Mahdavi M, Sharifpur M, Ahmadi MH, Meyer JP. 2019. Aggregation study of Brownian nanoparticles in convective phenomena. *J Therm Anal Calorim*. 135(1):111–121. doi:10.1007/s10973-018-7283-y
- Menni Y, Ghazvini M, Ameer H, Kim M, Ahmadi MH, Sharifpur M. 2020. Combination of baffling technique and high-thermal conductivity fluids to enhance the overall performances of solar channels. *Eng Computers* 1–22. doi:10.1007/s00366-020-01165-x
- Mesgarpour M, Mohebbi Najm Abad J, Alizadeh R, Wongwises S, Doranehgard MH, Ghaderi S, Karimi N. 2021. Prediction of the spread of Corona-virus carrying droplets in a bus-A computational based artificial intelligence approach. *J Hazard Mater*. 413:125358. doi:10.1016/j.jhazmat.2021.125358
- Miansari M, Nazari M, Toghraie D, Akbari OA. 2020. Investigating the thermal energy storage inside a double-wall tank utilizing phase-change materials (PCMs). *J Therm Anal Calorim*. 139(3):2283–2294. doi:10.1007/s10973-019-08573-2
- Milani Shirvan K, Mamourian M, Mirzakhani S, Ellahi R. 2016. Two phase simulation and sensitivity analysis of effective parameters on combined heat transfer and pressure drop in a solar heat exchanger filled with nanofluid by RSM. *J Mol Liq*. 220:888–901. doi:10.1016/j.molliq.2016.05.031
- Milani Shirvan K, Mamourian M, Mirzakhani S, Ellahi R. 2017. Numerical investigation of heat exchanger effectiveness in a double pipe heat exchanger filled with nanofluid: A sensitivity analysis by response surface methodology. *Powder Technol*. 313:99–111. doi:10.1016/j.powtec.2017.02.065
- Mostafaeipour A, Jahangiri M, Haghani A, Dehshiri SJH, Dehshiri SSH, Issakhov A, Sedaghat A, Saghaei H, Akinlabi ET, Sichilalu SM, et al. 2020. Statistical evaluation of using the new generation of wind turbines in South Africa. *Energy Rep*. 6:2816–2827. doi:10.1016/j.egy.2020.09.035
- Motamedi M, Mashhadi M, Rastgoo A. 2013. Vibration behavior and mechanical properties of carbon nanotube junction. *J Comp Theo Nano*. 10(4):1033–1037. doi:10.1166/jctn.2013.2803
- Motamedi M, Eskandari M, Yeganeh M. 2012. Effect of straight and wavy carbon nanotube on the reinforcement modulus in nonlinear elastic matrix nanocomposites. *Mater Des*. 34:603–608. doi:10.1016/j.matdes.2011.05.013
- Motamedi M, Naghdi AH, 2020. and SK. Jalali Effect of temperature on properties of aluminum/single-walled carbon nanotube nanocomposite by molecular dynamics simulation. *Proc Inst Mech Eng Part C: J Mech Eng Sci*. 234:635–642.
- Motamedi M, Naghdi A, Sohail A, Li Z. 2018. Effect of elastic foundation on vibrational behavior of graphene based on first-order shear deformation theory. *Adv Mech Eng*. 10(12):168781401881462. doi:10.1177/1687814018814624
- Nariman A, Kalbasi R, Rostami S. 2021. Sensitivity of AHU power consumption to PCM implementation in the wall-considering the solar radiation. *J Therm Anal Calorim*. 143(3):2789–2800. doi:10.1007/s10973-020-10068-4
- Nguyen Q, Bahrami D, Kalbasi R, Bach Q-V. 2020. Nanofluid flow through microchannel with a triangular corrugated wall: Heat transfer enhancement against entropy generation intensification. *Math Methods Appl Sci*. doi:10.1002/mma.6705
- Pahlavan S, Jahangiri M, Shamsabadi AA, Khechekhouche A. 2018. Feasibility study of solar water heaters in Algeria, a review. *J Solar Energy Res*. 3:135–146.
- Palacio M, Rincón A, Carmona M. 2020. Experimental comparative analysis of a flat plate solar collector with and without PCM. *Sol Energy* 206:708–721. doi:10.1016/j.solener.2020.06.047
- Ramakrishnan S, Wang X, Sanjayan J, Wilson J. 2017. Heat transfer performance enhancement of paraffin/expanded perlite phase change composites with graphene nanoplatelets. *Energy Proc*. 105:4866–4871. doi:10.1016/j.egypro.2017.03.964
- Rathore PKS, Shukla SK. 2019. Potential of macroencapsulated PCM for thermal energy storage in buildings: A comprehensive review. *Constr Build Mater*. 225:723–744. doi:10.1016/j.conbuildmat.2019.07.221
- Rostami S, Afrand M, Shahsavari A, Sheikholeslami M, Kalbasi R, Aghakhani S, Safdari Shadloo M, Oztop HF. 2020. A review of melting and freezing processes of PCM/Nano-PCM and their application in energy storage. *Energy* 211:118698. doi:10.1016/j.energy.2020.118698
- Rostami S, Kalbasi R, Jahanshahi R, Qi C, Abbasian-Naghnesh S, Karimipour A. 2020. Effect of silica nano-

- materials on the viscosity of ethylene glycol: An experimental study by considering sonication duration effect. *J Mater Res Technol.* 9(5):11905–11917. doi:[10.1016/j.jmrt.2020.07.105](https://doi.org/10.1016/j.jmrt.2020.07.105)
- Rostami S, Kalbasi R, Sina N, Goldanlou AS. 2021. Forecasting the thermal conductivity of a nanofluid using artificial neural networks. *J Therm Anal Calorim.* 145(4): 2095–2104. doi:[10.1007/s10973-020-10183-2](https://doi.org/10.1007/s10973-020-10183-2)
- Rostami S, Kalbasi R, Talebkeikhah M, Goldanlou AS. 2021. Improving the thermal conductivity of ethylene glycol by addition of hybrid nano-materials containing multi-walled carbon nanotubes and titanium dioxide: applicable for cooling and heating. *J Therm Anal Calorim.* 143(2): 1701–1712. doi:[10.1007/s10973-020-09921-3](https://doi.org/10.1007/s10973-020-09921-3)
- Sadeghi G, Nazari S, Ameri M, Shama F. 2020. Energy and exergy evaluation of the evacuated tube solar collector using Cu₂O/water nanofluid utilizing ANN methods. *Sustainable Energy Technol Assess.* 37:100578. doi:[10.1016/j.seta.2019.100578](https://doi.org/10.1016/j.seta.2019.100578)
- Saeed A, Karimi N, Hunt G, Torabi M. 2019. On the influences of surface heat release and thermal radiation upon transport in catalytic porous microreactors—a novel porous-solid interface model. *Chem Eng Process Intensification.* 143:107602. doi:[10.1016/j.cep.2019.107602](https://doi.org/10.1016/j.cep.2019.107602)
- Tian X-X, Kalbasi R, Jahanshahi R, Qi C, Huang H-L, Rostami S. 2020. Competition between intermolecular forces of adhesion and cohesion in the presence of graphene nanoparticles: Investigation of graphene nanosheets/ethylene glycol surface tension. *J Mol Liq.* 311: 113329. doi:[10.1016/j.molliq.2020.113329](https://doi.org/10.1016/j.molliq.2020.113329)
- Tian X-X, Kalbasi R, Qi C, Karimipour A, Huang H-L. 2020. Efficacy of hybrid nano-powder presence on the thermal conductivity of the engine oil: An experimental study. *Powder Technol.* 369:261–269. doi:[10.1016/j.powtec.2020.05.004](https://doi.org/10.1016/j.powtec.2020.05.004)
- Toghraie D, Sina N, Jolfaei NA, Hajian M, Afrand M. 2019. Designing an artificial neural network (ANN) to predict the viscosity of silver/ethylene glycol nanofluid at different temperatures and volume fraction of nanoparticles. *Phys A.* 534:122142. doi:[10.1016/j.physa.2019.122142](https://doi.org/10.1016/j.physa.2019.122142)
- Valizadeh Ardalan M, Alizadeh R, Fattahi A, Adelian Rasi N, Doranehgard MH, Karimi N. 2020. Analysis of unsteady mixed convection of Cu–water nanofluid in an oscillatory, lid-driven enclosure using lattice Boltzmann method. *J Therm Anal Calorim.* 1–17.
- Yan S-R, Kalbasi R, Karimipour A, Afrand M. 2021. Improving the thermal conductivity of paraffin by incorporating MWCNTs nanoparticles. *J Therm Anal Calorim.* 145(5):2809–2816. doi:[10.1007/s10973-020-09819-0](https://doi.org/10.1007/s10973-020-09819-0)
- Yan S-R, Kalbasi R, Nguyen Q, Karimipour A. 2020a. Rheological behavior of hybrid MWCNTs-TiO₂/EG nanofluid: A comprehensive modeling and experimental study. *J Mol Liq.* 308:113058. doi:[10.1016/j.molliq.2020.113058](https://doi.org/10.1016/j.molliq.2020.113058)
- Yan S-R, Kalbasi R, Nguyen Q, Karimipour A. 2020b. Sensitivity of adhesive and cohesive intermolecular forces to the incorporation of MWCNTs into liquid paraffin: Experimental study and modeling of surface tension. *J Mol Liq.* 310:113235. doi:[10.1016/j.molliq.2020.113235](https://doi.org/10.1016/j.molliq.2020.113235)
- Yang L, Huang J-n, Zhou F. 2020. Thermophysical properties and applications of nano-enhanced PCMs: An update review. *Energy Convers Manage.* 214:112876. doi:[10.1016/j.enconman.2020.112876](https://doi.org/10.1016/j.enconman.2020.112876)
- Yang YK, Kim MY, Chung MH, Park JC. 2019. PCM cool roof systems for mitigating urban heat island - An experimental and numerical analysis. *Energy Build.* 205: 109537. doi:[10.1016/j.enbuild.2019.109537](https://doi.org/10.1016/j.enbuild.2019.109537)
- Zhang H, Wu X, Wu Q, Xu S. 2019. Experimental investigation of thermal performance of large-sized battery module using hybrid PCM and bottom liquid cooling configuration. *Appl Therm Eng.* 159:113968. doi:[10.1016/j.applthermaleng.2019.113968](https://doi.org/10.1016/j.applthermaleng.2019.113968)